Available online at www.sciencedirect.com
ScienceDirect
Journal of Pharmaceutical and Biomedical Analysis 47 (2008) 260–267
JOURNAL OF PHARMACEUTICAL AND BIOMEDICAL ANALYSIS
www.elsevier.com/locate/jpba

Mechanism of interaction between human serum albumin and *N*-alkyl phenothiazines studied using spectroscopic methods

P.B. Kandagal, S.S. Kalanur, D.H. Manjunatha, J. Seetharamappa *

Department of Chemistry, Karnatak University, Dharwad 580 003, India

Received 1 November 2007; received in revised form 28 December 2007; accepted 3 January 2008
Available online 20 January 2008

Abstract

The binding characteristics of human serum albumin (HSA) with *N*-alkyl phenothiazines derivatives (NAP) *viz*., levomepromazine monomaleate (LMM) and propericiazine (PPC) have been studied by employing fluorescence, absorption, circular dichroism and FT-IR techniques. The Stern–Volmer quenching constant, K_{SV} values were found to decrease with increase in temperature thereby indicating the presence of static quenching mechanism in the interactions of NAP with HSA. The number of binding sites, n and the binding constant, K were noticed to be, respectively, 1.11 and $(5.188 \pm 0.034) \times 10^4\ M^{-1}$ for LMM and 1.06 and $(4.436 \pm 0.066) \times 10^4\ M^{-1}$ for PPC at 298 K. The negative value of enthalpy change and positive value of entropy change in the present study indicated that the hydrophobic forces played a major role in the binding of NAP to HSA. The circular dichroism and FT-IR spectral data revealed the conformational changes in the structure of protein upon its interaction with NAP. The binding distances and the energy transfer efficiency between NAP and protein were determined based on Förster's theory of energy transfer. The decreased binding constants of HAS–LMM and HAS–PPC systems in presence of common ions indicated the availability of higher concentration of free drug in plasma.
© 2008 Elsevier B.V. All rights reserved.

Keywords: Human serum albumin; Levomepromazine monomaleate; Propericiazine; Spectroscopic studies

1. Introduction

Human serum albumin (HSA), the most abundant human plasma protein contains a single polypeptide chain of 585 amino acids. It is largely helical (∼67%) and is composed of three structurally homologous domains (I, II and III) [1]. Each domain contains 10 helices; helices 1–6 form the respective sub-domains A and helices 7–10 comprise sub-domains B. Aromatic and heterocyclic ligands were found to bind within two hydrophobic pockets in sub-domains IIA and IIIA, namely sites I and II. Seven binding sites are localized for fatty acids in sub-domains IB, IIIA, IIIB and on the sub-domain interfaces [2]. HSA has a high affinity metal binding site at the N-terminus [3]. The multiple binding sites underlie the exceptional ability of HSA to interact with many organic and inorganic molecules and make this protein an important regulator of intercellular fluxes, as well as the pharmacokinetic behavior of many drugs [2,1].

Plasma protein binding of drugs assumes great importance since it influences their pharmacokinetic and pharmacodynamic properties, and may also cause interference with the binding of other endogenous and/or exogenous ligands as a result of overlap of binding sites and/or conformational changes. Therefore, detailed investigation of drug–protein interaction assumes significance for thorough understanding of the pharmacokinetic behavior of a drug and for the design of analogues with effective pharmacological properties. Hence, it becomes an important research field in chemistry, life sciences and clinical medicine.

Drug binding to HSA has been studied by numerous methods including immobilized affinity chromatography, equilibrium dialysis, affinity capillary electrophoresis, ultra filtration and ultracentrifugation [4–11]. However, these methods suffer from lack of sensitivity, long analysis time or reproducibility. It is not possible to get information with regard to the mechanism of quenching, transfer efficiency of energy, changes in conformation (secondary structure of protein) upon interaction, the microenvironment surrounding the fluorophore in the macromolecule, etc., by the above methods. However, spectroscopic techniques are ideal to obtain the above information and at the

* Corresponding author. Tel.: +91 836 2215286; fax: +91 836 2747884.
E-mail address: j_seetharam@rediffmail.com (J. Seetharamappa).

0731-7085/$ – see front matter © 2008 Elsevier B.V. All rights reserved.
doi:10.1016/j.jpba.2008.01.027

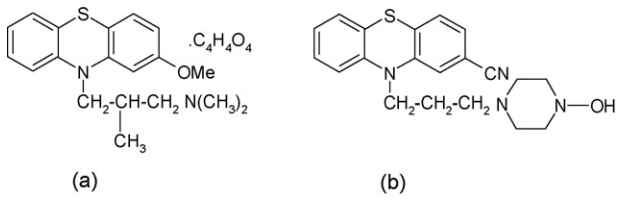

Fig. 1. Structure of (a) levomepromazine monomaleate and (b) propericiazine.

same time they are known for accuracy, sensitivity, rapidity and convenience of usage. Hence, spectroscopic techniques have been widely applied in investigating drug binding with albumin under physiological conditions.

N-alkyl phenothiazines derivatives (NAP) *viz*., levomepromazine monomaleate (LMM) and propericiazine (PPC) (Fig. 1a and b) an important class of tricyclic phenothiazine compounds are widely used as anticholinergic, antihistaminic and antipsychotic drugs [12]. Some aspects of binding of a few tricyclic compounds to plasma proteins have been reported [13–15]. However, attempts have not been made so far to investigate the interactions of LMM and PPC with HSA. The present study is focused on interactions of NAP with HSA. This is the first report on the mechanism of interaction of LMM and PPC with HSA employing fluorescence spectroscopy, UV–vis absorption spectroscopy, FT-IR and CD methods.

2. Experimental

2.1. Equipments and spectral measurements

Fluorescence measurements were performed on a Hitachi spectrofluorimeter Model F-2000 (Tokyo, Japan) equipped with a 150W Xenon lamp and a slit width of 5 nm. The CD measurements were made on a JASCO-J-715 spectropolarimeter (Tokyo, Japan). The infrared spectra were acquired on a Thermo Nicolet-5700 FT-IR spectrometer (Waltham, MA, USA) equipped with a germanium attenuated total reflection (ATR) accessory, a DTGS KBr detector and a KBr beam splitter. All spectra were recorded via the ATR method with a resolution of 4 cm^{-1} and 60 scans. The absorption spectra were recorded on a double beam Varian CARY 50-BIO UV–vis spectrophotometer (Mulgrave Victoria, Australia) equipped with a 150W Xenon lamp and a slit width of 5 nm.

2.2. Reagents

Essentially fatty acid free HSA was obtained from Sigma Chemical Company (St. Louis, USA). Levomepromazine monomaleate and propericiazine were obtained as gift samples from M/s A.G. Bayer, Leverkusen and Byk Gulden Pharmaceuticals (Germany). The solutions of NAP and HSA were prepared in 0.1 M phosphate buffer of pH 7.4 containing 0.15 M NaCl. HSA solution was prepared based on its molecular weight of 66,000. Site probes *viz*., warfarin, ibuprofen and digitoxin were initially dissolved in minimum amount of methanol and then diluted with distilled water. All other materials were of analytical reagent grade and double distilled water was used throughout.

2.3. Procedures

2.3.1. NAP–HSA interactions

Fluorescence measurements were carried out by keeping the concentration of HSA fixed at 5 μM and that of NAP was varied from 10 to 60 μM. Fluorescence spectra were recorded at 288, 298 and 308 K in the range of 300–500 nm upon excitation at 280 nm in each case ($n = 3$ replicates).

2.3.2. Circular dichroism (CD) measurements

The CD spectra of HSA (5 μM) in presence and absence of NAP were recorded in the range of 200–250 nm using a 0.1 cm cell at 0.2 nm intervals with three scans averaged for each CD spectra. The molar ratios of HSA to drug maintained were 1:4 and 1:8 for HAS–LMM and 1:2 and 1:4 for HAS–PPC.

2.3.3. FT-IR measurements

The FT-IR spectra of HSA (5 μM) in presence and absence of NAP were recorded ($n = 3$ replicates) in the range of 1500–1700 cm^{-1}. The molar ratio of HSA to drug was maintained at 1:4. The corresponding absorbance contributions of buffer and free NAP solutions were recorded and digitally subtracted with the same instrumental parameters.

2.3.4. Energy transfer between protein and NAP

The absorption spectrum of NAP (5 μM) was recorded in the range of 300–500 nm ($n = 3$ replicates). The emission spectrum of HSA (5 μM) was also recorded in the range of 300–500 nm ($n = 3$ replicates). Then, the overlap of the UV absorption spectrum of NAP with the fluorescence emission spectrum of HSA was used to calculate the energy transfer.

2.3.5. Displacement experiments

The displacement experiments ($n = 3$ replicates) were performed using the site probes *viz*., warfarin, ibuprofen and digitoxin by keeping the concentration of HSA and probe constant (each of 5 μM). The fluorescence quenching titration was used as before to determine the binding constants of NAP–HSA systems in presence of the above site probes for sites I, II and III.

2.3.6. Absorption measurements

The absorption spectra of HSA in presence and absence of NAP were noted down in the range of 200–320 nm ($n = 3$ replicates). HSA concentration was fixed at 5 μM while that of NAP was varied from 10 to 50 μM.

2.3.7. Effects of common ions

The fluorescence spectra of NAP–HSA were recorded in presence and absence of various common ions *viz*., Cu^{2+}, Ni^{2+}, Zn^{2+}, Ca^{2+} and Co^{2+} in the range of 300–500 nm upon excitation at 280 nm ($n = 3$ replicates). The concentrations of HSA and common ion were fixed at 5 and 6 μM, respectively.

3. Results and discussion

3.1. Analysis of fluorescence quenching of HSA by NAP

Fluorescence quenching is the decrease of the quantum yield of fluorescence from a fluorophore induced by a variety of molecular interactions with a quencher molecule. Generally, the fluorescence of HSA comes from tryptophan, tyrosine and phenylalanine residues. The intrinsic fluorescence of HSA is almost due to tryptophan alone because phenylalanine has a very low quantum yield and the fluorescence of tyrosine is almost totally quenched if it is ionized or near an amino group, a carboxyl group or a tryptophan. This viewpoint was well supported by the experimental observations of Sulkowska [16]. That is, the change of intrinsic fluorescence intensity of HSA was due to tryptophan residue when small molecules bound to HSA. When different amounts of drug solution were titrated with a fixed concentration of HSA, a remarkable decrease in the fluorescence intensity of HSA was observed with both LMM and PPC (Fig. 2A and B) in the present study. The emission wavelength of HSA was shifted from 336 to 333 nm indicating that the chromophore of protein was placed in a more hydrophobic environment after the addition of LMM [17]. Under the experimental conditions, LMM did not show any fluorescence intensity. PPC was observed to be weakly fluorescent (Fig. 2B). A red shift in maximum emission wavelength of HSA (from 336 to 350 nm) was observed upon the addition of PPC probably due to the loss of the compact structure of hydrophobic sub-domain

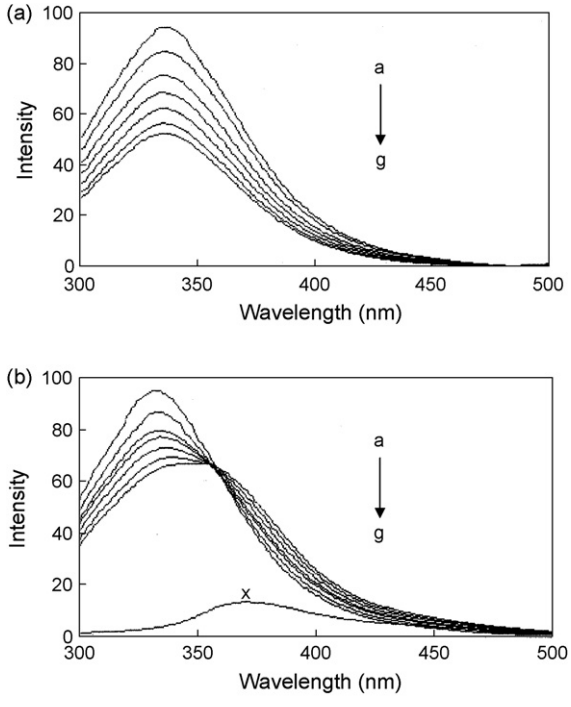

Fig. 2. (A) Fluorescence spectra of HSA in presence of LMM. Concentration of HSA was fixed at 5 μM (a) while that of LMM was maintained at 10 (b), 20 (c), 30 (d), 40 (e), 50 (f) and 60 μM (g). (B) Fluorescence spectra of HSA in presence of PPC. Concentration HSA was fixed at 5 μM (a) while that of PPC was maintained at 10 (b), 20 (c), 30 (d), 40 (e), 50 (f) and 60 μM (g). The concentration of PPC alone was 10 μM (x).

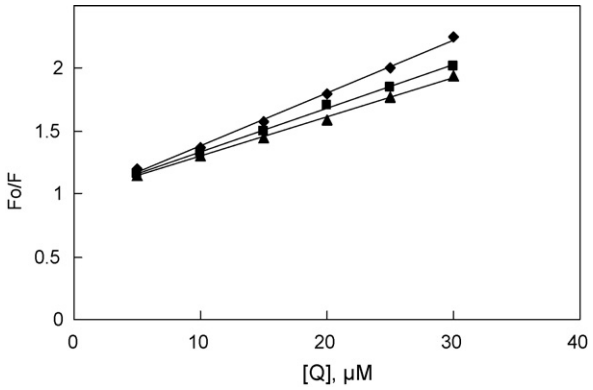

Fig. 3. Stern–Volmer plot for the binding of PPC with HSA at 288 (♦), 298 (■) and 308 K (▲).

where tryptophan was placed [16]. PPC exhibited maximum emission wavelength at 368 nm. Further, the occurrence of an isoactinic point at 355 nm revealed the existence of bound and free PPC in equilibrium [18]. In other words, an isoactinic point was considered as a direct evidence for drug–protein complex.

3.2. Binding parameters and mechanism

Quenching can be induced by dynamic and static process. Dynamic and static quenching can be distinguished based on their differences on temperature dependence. Higher temperature results in faster diffusion and larger amounts of collisional quenching. It will typically lead to the dissociation of weakly bound complexes and smaller amounts of static quenching. Therefore, the quenching constant increases for dynamic quenching while it decreases for static quenching with increase in temperature. The possible quenching mechanism can be deduced from the Stern–Volmer plot. The Stern–Volmer plot for a representative drug–HSA system is shown in Fig. 3. The Stern–Volmer plots were observed to be linear for NAP–HSA with the slopes decreasing with increase in temperatures. The values of K_{SV} and R^2 at different temperatures were evaluated and the same are given in Table 1. The values of K_{SV} at different temperatures indicated the presence of static quenching mechanism in the interaction between NAP and HSA. In order to invoke this possibility, the mechanism was assumed to involve dynamic quenching. The equation for dynamic quenching is presented by [19]:

$$\frac{F_0}{F} = 1 + K_q\tau_0[Q] = 1 + K_{SV}[Q] \quad (1)$$

where F and F_0 are the fluorescence intensities with and without quencher, respectively. K_q, K_{SV}, τ_0 and $[Q]$ are the quenching rate constant, the dynamic quenching constant, the average lifetime of the biomolecule without quencher and the concentration of quencher, respectively. Obviously,

$$K_{SV} = \frac{K_q}{t_0} \quad (2)$$

Since the fluorescence lifetime of the biopolymer is 10^{-8} s [20], the quenching rate constant, K_q can be calculated using

Table 1
Thermodynamic and binding parameters of NAP–HSA systems

Drug	T (K)	K_{SV} ($\times 10^{-4}$ M^{-1})	R^2	Binding constant, K ($\times 10^{-4}$ M^{-1})	n	K_q ($\times 10^{-12}$ M^{-1} S^{-1})	ΔG^0 (kJ mol^{-1})	ΔH^0 (kJ mol^{-1})	ΔS^0 (J mol^{-1} K^{-1})
LMM	288	2.26 ± 0.022	0.9970	6.982 ± 0.062	1.13	2.26 ± 0.022	−26.71	−20.15	+22.78
	298	1.81 ± 0.039	0.9969	5.188 ± 0.034	1.11	1.81 ± 0.039	−26.90		
	308	1.30 ± 0.024	0.9955	3.990 ± 0.055	1.03	1.30 ± 0.024	−27.13		
PPC	288	4.22 ± 0.052	0.9980	5.688 ± 0.049	1.10	4.22 ± 0.052	−26.22	−12.58	+47.21
	298	3.46 ± 0.041	0.9988	4.436 ± 0.066	1.06	3.46 ± 0.041	−26.51		
	308	3.12 ± 0.055	0.9983	3.655 ± 0.091	1.01	3.12 ± 0.055	−26.90		

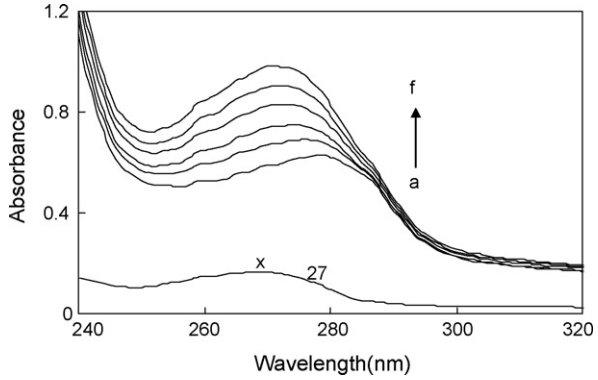

Fig. 4. Absorbance spectra of HSA, PPC and HAS–PPC system. HSA concentration was 5 μM (a). PPC concentration for PPC–HSA system was maintained at 10 (b), 20 (c), 30 (d), 40 (e) and 50 μM (f). The concentration of PPC alone was 5 μM (x).

the above equation. The values of K_q are given in Table 1. The maximum scatter collision quenching constant, K_q of various quenchers with the biopolymer [21] is reported to be 2×10^{10} L M^{-1} S^{-1}. The order of magnitude of K_q was calculated to be 10^{12} for both LMM–HSA and PPC–HSA systems in the present study. So, the rate constants of the protein quenching procedure initiated by LMM and PPC are greater than the value of K_q for the scatter mechanism. This implied that the quenching was not initiated by dynamic collision but originated from the formation of a complex.

3.3. Changes of the protein's secondary structure induced by drug binding

In order to obtain more information on NAP–HSA interactions, UV absorption spectra of drug, HSA and drug–HSA systems were recorded. It was observed that the absorption of HSA increased regularly upon the successive addition of NAP. The maximum peak position of LMM–HSA was shifted slightly towards higher wavelength region. This indicated the change in polarity around the tryptophan residue and the change in peptide strand of HSA molecules and hence the change in hydrophobicity [22,23]. So, the binding of LMM to protein molecule might lead to change in conformation of the protein [24]. For PPC, a blue shift of maximum peak position (Fig. 4) was noticed due to formation of a complex between the drug and HSA [22]. This also indicated that the peptide strands of protein molecules extended further more upon the addition of PPC to HSA [22].

In order to understand the physicochemical properties of NAP governing its spectral behavior and to draw relevant conclusions on the NAP–HSA binding mechanism, CD measurements were performed on HSA and NAP–HSA systems. The CD spectra of HSA in presence and absence of a representative drug, PPC are given in Fig. 5. The HSA exhibited two negative bands, which are characteristic of α-helix structure of the protein [25] in UV region at 209 ± 1 and 220 ± 2 nm. The reasonable explanation is that the negative peaks between 208 and 209 nm and 222–223 nm are both contributed to $n \rightarrow \pi^*$ transfer for the peptide bond of α-helix [26]. Appreciable changes in the conformation of HSA in terms of α-helicity were not noticed with lower concentration

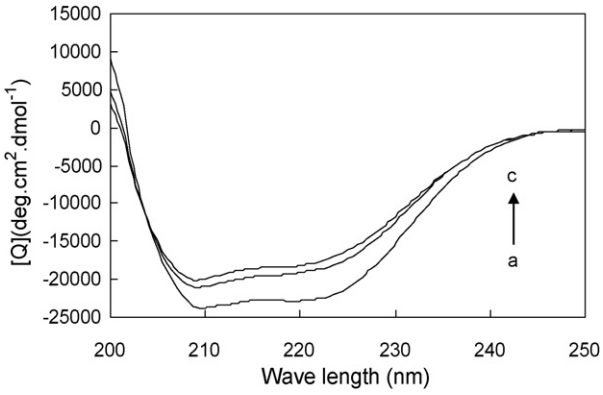

Fig. 5. The CD spectra of the HAS–PPC system. HSA concentration was fixed at 5 μM (a). In HAS–PPC system, the PPC concentration was maintained at 10 (b) and 20 μM (c).

of NAP. However, noticeable changes in α-helicity values were observed in presence of higher concentrations of both NAP.

The CD results were expressed in terms of mean residue ellipticity (MRE) in deg cm^2 $dmol^{-1}$ according to the equation [27]:

$$\text{MRE} = \frac{\text{Observed CD (mdeg)}}{C_P n l \times 10} \quad (3)$$

where C_P is the molar concentration of the protein, n is the number of amino acid residues and l is the path length. The α-helical contents of free and bound HSA were calculated from MRE value at 208 nm using the equation [27]:

$$\alpha\text{-Helix (\%)} = \frac{[-\text{MRE}_{208} - 4000]}{[33,000 - 4000]} \times 100 \quad (4)$$

where MRE_{208} is the observed MRE value at 208 nm, 4000 is the MRE of the β-form and random coil conformation cross at 208 nm and 33,000 is the MRE value of a pure α-helix at 208 nm. As evident from Fig. 5, the interaction of the drug with HSA decreased the intensity of the far-UV CD bands without causing any significant shift of the peaks. Further, the results revealed that the α-helicity was decreased from (63.74 ± 0.7)% in free HSA to (48.62 ± 0.8)% in HAS–LMM complex and from (63.74 ± 0.6)% in free HSA to (54.2 ± 0.8)% in HAS–PPC complex. The CD spectra of HSA in presence and absence of NAP were observed to be similar in shape indicating that the structure of HSA was also predominantly α-helical [28] even after binding to NAP.

Additional evidence regarding NAP–HSA interactions was obtained from FT-IR spectroscopic results. Infrared spectra of a protein exhibit a number of the so-called amide bands, which represent different vibrations of the peptide moiety. Of all the amide modes of the peptide group, the single most widely used one in studies of protein secondary structures is the amide I. The amides I and II peak occur in the region of 1600–1700 cm^{-1} and 1500–1600 cm^{-1}, respectively. Amide I band is more sensitive to the changes in protein secondary structure compared to amide II. Hence, the amide I band is more useful for the studies of secondary structure [29–32]. In the amide I region, the observed stretching frequency of C=O hydrogen bonded to NH moieties

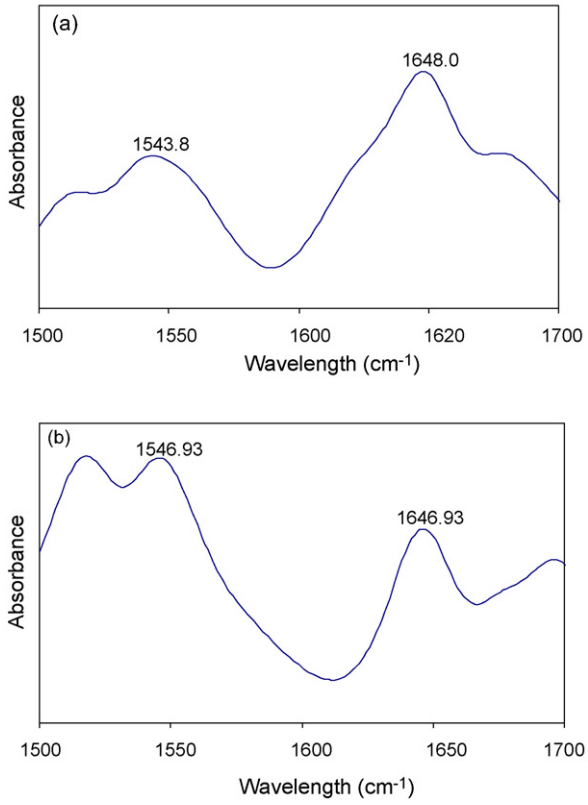

Fig. 6. FT-IR spectra and difference spectra of HSA; (a) the FT-IR spectra of free HSA (subtracting the absorption of the buffer solution from the spectrum of the protein solution) and (b) the FT-IR difference spectra of HSA (subtracting the absorption of the PPC-free form from that of PPC–HSA bound form) in phosphate buffer; $C_{HSA} = 5.0$ and $C_{PPC} = 20$ μM.

is dependent upon the secondary structure adopted by the peptide chain. Changes in the structure of the protein are reflected by changes in the component band positions of the amide I region [33]. The FT-IR spectra of free HSA (Fig. 6a) and its PPC complex (Fig. 6b) in phosphate buffer solution were recorded at 298 K. The peak positions of amides I and II were found to be shifted upon the addition of NAP to HSA. The amide I band was shifted from 1648 ± 0.5 to 1650 ± 0.6 cm^{-1} for LMM and from 1648 ± 0.3 to 1646.23 ± 0.6 cm^{-1} for PPC while the amide II peak was shifted from 1543.4 ± 0.7 to 1542.2 ± 0.9 cm^{-1} for LMM and from 1543.4 ± 0.5 to 1546.65 ± 0.7 cm^{-1} for PPC. These results indicated that both the NAP interacted with the C=O and CN groups in the protein polypeptides. The NAP–protein complexes caused the rearrangement of the polypeptide carbonyl hydrogen-bonding network and finally the reduction of the protein α-helical structure.

3.4. Apparent binding constant and binding sites

When small molecules bind independently to a set of equivalent sites on a macromolecule, the equilibrium between free and bound molecules could be represented by the equation [22]:

$$\log\frac{(F_0 - F)}{F} = \log K + n \log[Q] \quad (5)$$

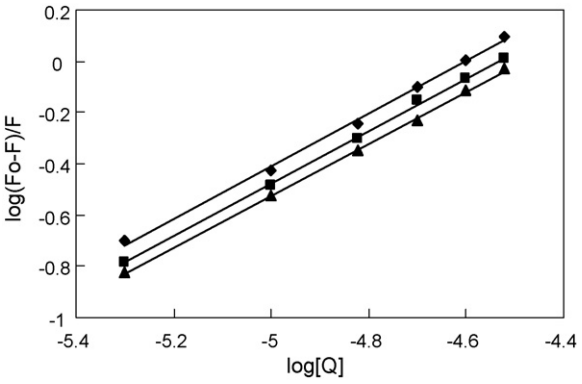

Fig. 7. The plot of $\log(F_0 - F)/F$ vs. $\log[Q]$ for quenching of HSA by PPC at 288 (♦), 298 (■), 308 K (▲); c(PPC) = 10–60 μM; c(HSA) = 5 μM.

where K and n are the binding constant and number of binding sites, respectively. The values of K and n for LMM–HSA and PPC–HSA systems were calculated from the intercept and slope of the plot of $\log(F_0 - F)/F$ *versus* $\log[Q]$ and the same plot for a representative system, PPC–HSA is given in Fig. 7. The value of K is significant to understand the distribution of the drug in plasma since the weak binding can lead to a short lifetime or poor distribution, while strong binding can decrease the concentrations of free drug in plasma. The values of K and n are summarized in Table 1. It was noticed that the binding constant values decreased with increase in temperature due to reduction of the stability of NAP–HSA complexes. The value of n is helpful to know the number of binding sites and to locate the binding site in HSA for the drug. The values of n for LMM–HSA and PPC–HSA were noticed to be almost unity indicating that there was one independent class of binding sites on HSA for both NAP. Hence, the NAP most likely bound to the hydrophobic pocket located in sub-domain IIA; that is to say Trp 214 is near or within the binding site [27].

Sudlow et al. [34] have suggested two main distinct binding sites (sites I and II) in HSA. Sites I and II of HSA show affinity for warfarin and ibuprofen, respectively. It is reported that digitoxin binding is independent of sites I and II [35] and binds to site III. In order to establish the binding site in HSA for NAP, displacement experiments were performed using site probes, warfarin, ibuprofen, digitoxin. For this, emission spectra of ternary mixtures of NAP, HSA and site probe were recorded. The corresponding binding constant values were evaluated and these are recorded in Table 2. The binding constants of NAP–HSA decreased remarkably upon the addition of warfarin while these remained almost same with the addition of ibuprofen/digitoxin. These results revealed that warfarin displaced both LMM and PPC from the binding site while ibuprofen and digitoxin had a little effect on the binding of NAP to HSA. Hence, we have concluded that the NAP were bound to site I of HSA.

3.5. Thermodynamic parameters

The thermodynamic parameters, enthalpy change (ΔH^0) and entropy change (ΔS^0) of NAP–HSA interaction are important for confirming binding mode. For this purpose, the temperature dependence of binding constant was studied. Binding studies were carried out at 288, 298 and 308 K at which HSA does not under go any structural degradation. The molecular forces contributing to protein interactions with small molecular substrates may include van der Waals interactions, hydrogen bonds, electrostatic and hydrophobic interactions and so on [22]. The thermodynamic parameters were evaluated using the equations:

$$\log K = \frac{-\Delta H^0}{2.303RT} + \frac{\Delta S^0}{2.303R} \quad (6)$$

$$\Delta G^0 = \Delta H^0 - T\Delta S^0 \quad (7)$$

The plot of $\log K$ *versus* $1/T$ enabled the determination of the values of ΔH^0 and ΔS^0. Ross and Subramanian [36] have characterized the sign and magnitude of the thermodynamic parameters associated with various individual kinds of interaction. For typical hydrophobic interactions, both ΔH^0 and ΔS^0 are positive, while these are negative for van der Waals forces and hydrogen-bond formation in low dielectric media [36,37]. Moreover, the specific electrostatic interaction between ionic species in an aqueous solution is characterized by positive ΔS^0 value and negative ΔH^0 value (small). For NAP–HSA complexes, the main source of ΔG^0 value was derived from a large contribution of ΔS^0 term with a little contribution from ΔH^0 factor. So, the main interaction between NAP and HSA was believed to be hydrophobic. However, the electrostatic interaction could not be excluded.

3.6. Energy transfer from HSA to NAP

Fluorescence resonance energy transfer (FRET) is a distance dependent interaction between the different electronic excited states of molecules in which excitation energy is transferred from one molecule (donor) to another molecule (acceptor) without emission of a photon from the former molecular system. The efficiency of FRET depends mainly on the following factors: (i) the extent of overlap between the donor emission and the acceptor absorption (ii) the orientation of the transition dipole of donor and acceptor and (iii) the distance between the donor and acceptor. The spectral overlap between the fluorescence emission spectrum of free HSA and absorption spectrum of a representative drug, PPC is shown in Fig. 8.

The efficiency of energy transfer, E was determined according to Förster's energy transfer theory [38]. The value of E was calculated using the equation:

$$E = 1 - \frac{F}{F_0} = \frac{R_0^6}{R_0^6 + r^6} \quad (8)$$

where F and F_0 are the fluorescence intensities of HSA in presence and absence of NAP, r is the distance between acceptor and donor and R_0 is the critical distance when the transfer efficiency is 50%. The value of R_0 was evaluated using the equation:

$$R_0^6 = 8.8 \times 10^{-25} k^2 N^{-4} \Phi J \quad (9)$$

where k^2 is the spatial orientation factor of the dipole, N is the refractive index of the medium, Φ is the fluorescence quantum

Table 2
Comparison of the binding constant of NAP–HSA before and after the addition of the site probe

Drug	K, without the site probe ($\times 10^{-4}$ M^{-1})	K, with warfarin ($\times 10^{-4}$ M^{-1})	K, with Ibuprofen ($\times 10^{-4}$ M^{-1})	K, with digitoxin ($\times 10^{-4}$ M^{-1})
LMM	5.188 ± 0.025	4.068 ± 0.012	5.082 ± 0.017	5.245 ± 0.028
PPC	4.436 ± 0.031	3.635 ± 0.023	4.281 ± 0.026	4.386 ± 0.033

yield of the donor and J is the overlap integral of the fluorescence emission spectrum of the donor and the absorption spectrum of the acceptor. J is given by

$$J = \frac{\Sigma F(\lambda)\varepsilon(\lambda)\lambda^4 \Delta\lambda}{\Sigma F(\lambda)\Delta\lambda} \quad (10)$$

where $F(\lambda)$ is the fluorescence intensity of the fluorescent donor of wavelength, λ, $\varepsilon(\lambda)$ is the molar absorption coefficient of the acceptor at wavelength, λ. In the present case, $K^2 = 2/3$, $N = 1.36$ and $\Phi = 0.118$ [27]. From equations (8)–(10), we could calculate that $J = 1.14 \times 10^{-16}$ cm^3 L mol^{-1}, $E = 0.24$, $R_0 = 2.57$ nm, and $r = 3.11$ nm for LMM–HSA system and, $J = 1.04 \times 10^{-16}$ cm^3 L mol^{-1}, $E = 0.32$, $R_0 = 2.53$ nm and $r = 2.87$ nm for PPC–HSA system. The average distance of 2–8 nm between a donor and acceptor indicated that the energy transfer from HSA to NAP occurred with high probability [39]. The larger value of r compared to that of R_0 in the present study also revealed the presence of static type quenching mechanism [18].

3.7. Effects of other ions on the interactions of NAP with HSA

In plasma, there are some metal ions, which can affect the reactions of the drugs and serum albumins. Trace metal ions, especially the bivalent type are essential in the human body and play an important structural role in many proteins. It is reported [40] that Cu^{2+}, Zn^{2+}, Ni^{2+}, Co^{2+} and Ca^{2+} and other metal ions can form complexes with serum albumins. Hence, the effects of some metal salt solutions *viz.*, $CuCl_2$, $ZnCl_2$, $NiCl_2$, $CoCl_2$ and $CaCl_2$ on the binding of NAP with HSA were investigated in the present study. The binding constants of NAP–HSA in presence of above ions were evaluated and these results are shown in Table 3. The binding constants of LMM–HSA and PPC–HSA

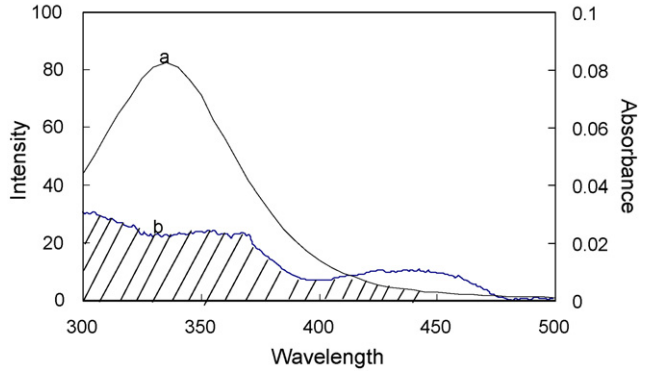

Fig. 8. The overlap of the fluorescence spectrum of HSA (a) and the absorbance spectrum of PPC (b). {c(HSA)/c(PPC) = 1:1}.

Table 3
Effects of common ions on binding constants of NAP–HSA systems

System	Binding constant (M^{-1})	
	LMM	PPC
HAS	$(5.188 \pm 0.034) \times 10^4$	$(4.436 \pm 0.034) \times 10^4$
HSA + Cu^{2+}	$(4.436 \pm 0.034) \times 10^4$	$(2.506 \pm 0.066) \times 10^4$
HSA + Zn^{2+}	$(3.349 \pm 0.034) \times 10^4$	$(2.208 \pm 0.034) \times 10^4$
HSA + Ni^{2+}	$(3.326 \pm 0.034) \times 10^4$	$(2.824 \pm 0.034) \times 10^4$
HSA + Co^{2+}	$(2.831 \pm 0.034) \times 10^4$	$(2.118 \pm 0.034) \times 10^4$
HSA + Ca^{2+}	$(3.155 \pm 0.034) \times 10^4$	$(2.103 \pm 0.034) \times 10^4$

systems decreased in various degrees in presence of Cu^{2+}, Zn^{2+}, Ni^{2+}, Co^{2+} and Ca^{2+}. This was likely to be caused by a conformational change in the vicinity of the binding site. The decrease in the binding constant in presence of above metal ions would shorten the storage time of the drug in blood plasma and hence more amount of free drug would be available in plasma [24]. This led to the need for more doses of NAP to achieve the desired therapeutic effect in presence of above ions.

4. Conclusions

In the present work, the binding of NAP to HSA was carried out employing spectroscopic techniques under physiological conditions. Various binding parameters have been evaluated. The decreased values of K with increase in temperature indicated the presence of static quenching mechanism. The values of n revealed the presence of a single class of binding site on HSA for NAP. Thermodynamic parameters indicated that the hydrophobic interactions played a major role in the interactions of NAP with HSA. The distance r between NAP and HSA was obtained based on fluorescence resonance energy transfer. The spectroscopic results revealed the changes in the secondary structure of HSA in presence of NAP. The decreased K values of NAP–HSA complexes in presence of common ions indicated the availability of higher concentrations of free drug. Since, the pharmaceutical firms need standardized screens for HSA binding in the first step of new drug design, this kind of study of interaction between HSA with NAP would be useful in pharmaceutical industry, chemistry, life sciences and clinical medicine.

Acknowledgements

The authors thank the Department of Science and Technology, New Delhi, India for financial support to this work. Thanks are also due to Prof. M.R.N. Murthy, Indian Institute of Science, Bangalore, for CD facilities and also to the authorities of the Karnatak University, Dharwad for extending the necessary facilities.

References

[1] H.M. He, D.C. Carter, Nature 358 (1992) 209–215.
[2] T. Peters, All About Albumin. Biochemistry Genetics and Medical Applications, Academic Press, San Diego, 1996.
[3] D.C. Carter, J.X. Ho, Adv. Protein. Chem. 45 (1994) 153–203.
[4] H. Seung Kim, D.S. Hage, J. Chromatogr. B 816 (2005) 57–66.
[5] H.S. Kim, R. Mallik, D.S. Hage, J. Chromatogr. B 837 (2006) 138–146.
[6] U.K. Hansen, E. Dørge, A.O. Pedersen, Anal. Biochem. 340 (2006) 145–153.
[7] M. Vita, M.A. Rehim, C. Nilsson, Z. Hassan, P. Skansen, H. Wan, L. Meurling, M. Hassan, J. Chromatogr. B 821 (2005) 75–80.
[8] L.W. Zhang, K. Wang, X.X. Zhang, Anal. Chim. Acta 603 (2007) 101–110.
[9] M.A.M. Gómez, M.M.C. Avilés, S. Sagrado, R.M.V. Camañas, M.J.M. Hernández, J. Chromatogr. A 1147 (2007) 261–269.
[10] J. Oravcova, B. Bobs, W. Lindner, J. Chromatogr. B 677 (1996) 1–28.
[11] D.E. Epps, T.J. Raub, V. Caiolfa, A. Chiari, M. Zamai, J. Pharm. Pharmacol. 51 (1998) 41–48.
[12] J. Seetharamappa, N. Motohashi, D.K. Demertzi, Current Drug Targets 7 (2006) 1107–1121.
[13] H. Aki, M. Yamamoto, J. Pharm. Pharmacol. 41 (1989) 674–678.
[14] T. Miyoshi, K. Sukimoto, M. Otagiri, J. Pharm. Pharmacol. 44 (1992) 28–33.
[15] T. Maruyama, M. Otagiri, A. Takadate, Chem. Pharm. Bull. 38 (1990) 1688–1692.
[16] A. Sulkowska, J. Mol. Struct. 614 (2002) 227–232.
[17] T. Yuan, A.M. Weljie, H.J. Vogel, Biochemistry 37 (1998) 3187–3192.
[18] W. He, Y. Li, C. Xue, Z. Hu, X. Chen, F. Sheng, Bioorg. Med. Chem. 13 (2005) 1837–1845.
[19] J.R. Lakowicz, Principles of Fluorescence Spectroscopy, second ed., Plenum Press, New York, 1999, 237-265.
[20] G.Z. Chen, X.Z. Huang, J.G. Xu, Z.Z. Zheng, Z.B. Wang, The Methods of Flourescence Analysis, second ed., Beijing Science Press, 1990, 2-39.
[21] J.R. Lakowica, G. Weber, Biochemistry 12 (1973) 4161–4170.
[22] K.H. Ulrich, Pharmacol. Rev. 33 (1981) 17–53.
[23] W.S. Tao, Protein Molecular Basic, The People's Education Press, 1981, 256.
[24] F.L. Cui, J. Fan, J.P. Li, Z. Hu, Bioorg. Med. Chem. 12 (2004) 151–157.
[25] L.T. Lemiesz, A. Karaczyn, B.K. Keppler, H. Koztowski, J. Inorg. Biochem. 78 (2000) 341–346.
[26] P. Yang, F. Gao, The Principle of Bioinorganic Chemistry, Science Press, 2002, 349.
[27] G. Hong, L. Liandi, L. Jiaqin, Q. Kong, C. Xingguo, Z. Hu, J. Photochem. Photobiol. Part A 167 (2004) 213–221.
[28] Y.J. Hu, L. Yi, S.X. Song, F.X. Yang, Q.S. Sheng, J. Mol. Struct. 738 (2005) 145–149.
[29] S. Wi, P. Pancoka, T.A. Keiderling, Biospectroscopy 4 (1998) 93–106.
[30] K. Rahmelow, W. Hubner, Anal. Biochem. 241 (1996) 5–13.
[31] S.Y. Lin, Y.S. Wei, M.J. Li, S.L. Wang, Eur. J. Pharm. Biopharm. 57 (2004) 457–464.
[32] J.W. Brauner, C.R. Flach, R. Mendeisohn, J. Am. Chem. Soc. 127 (2005) 100–109.
[33] P.M. Bummer, Int. J. Pharm. 132 (1996) 143–151.
[34] G. Sudlow, D.J. Birkett, D.N. Wade, Mol. Pharmacol. 12 (1976) 1052–1061.
[35] I. Sjoholm, B. Ekman, A. Kober, I.L. Pahlman, B. Seiving, T. Sjodin, Mol. Pharmacol. 16 (1979) 767–777.
[36] P.D. Ross, S. Subramanian, Biochemistry 20 (1981) 3096–3102.
[37] A. Mallick, B. Haldar, N. Chattopadhyay, J. Phys. Chem. B 109 (2005) 14683–14690.
[38] T. Förster, O. Sinanoglu (Eds.), Modern Quantum Chemistry, vol. 3, Academic Press, New York, 1996, p. 93.
[39] Y.J. Hu, Y. Liu, L.X. Zhang, J. Mol. Struct. 750 (2005) 174–178.
[40] G. Zhang, Y. Wang, H. Zhang, S. Tang, W. Tao, Pest. Biochem. Physiol. 87 (2007) 23–29.